Euler–Bernoulli type beam theory for elastic bodies with nonlinear response in the small strain range

A. JANEČKA[1)], V. PRŮŠA[1)], K. R. RAJAGOPAL[2)]

[1)] *Faculty of Mathematics and Physics*
Charles University in Prague
Sokolovská 83
Praha 8 – Karlín
CZ 186 75, Czech Republic
e-mails: janecka@karlin.mff.cuni.cz, prusv@karlin.mff.cuni.cz

[2)] *Texas A&M University*
Department of Mechanical Engineering
3123 TAMU
College Station TX 77843-3123, U.S.A.
e-mail: krajagopal@tamu.edu

The response of many new metallic alloys as well as ordinary materials such as concrete is elastic and nonlinear even in the small strain range. Thus, using the classical linearized theory to determine the response of bodies could lead to a miscalculation of the stresses corresponding to the given strains, even in the small strain regime. As stresses can determine the failure of structural members, such miscalculation could be critical. We investigate the quantitative impact of the material nonlinearity in the Euler–Bernoulli type beam theory. The governing equations for the deflection are found to be nonlinear integro-differential equations, and the equations are solved numerically using a variant of the spectral collocation method. The deflection and the spatial stress distribution in the beam have been computed for two sets of models, namely the standard linearized model and some recent nonlinear models used in the literature to fit experimental data. The predictions concerning the deflection and the spatial stress distribution based on the standard linearized model and the nonlinear models are considerably different.

Key words: Euler–Bernoulli beam theory, nonlinear elasticity, small strain, implicit constitutive relations, spectral collocation method.
Mathematics Subject Classification: 74B20, 65N35.

1. Introduction

A NEW CLASS OF CONSTITUTIVE RELATIONS for elastic solids wherein the stress $\mathbb{T}$ and the deformation gradient $\mathbb{F}$ are related by an implicit relation $\mathfrak{f}(\mathbb{T}, \mathbb{F}) = \mathbb{0}$ has been introduced by RAJAGOPAL [1, 2]. These implicit models have been shown to be suitable in describing the response of various elastic materials, in

particular soft tissues, see for example Freed and Einstein [3] and Freed [4]. An interesting subclass of models of type $\mathfrak{f}(\mathbb{T}, \mathbb{F}) = \mathbb{0}$ are models for isotropic elastic bodies defined through

$$(1.1) \qquad \mathbb{B} = \alpha_0 \mathbb{I} + \alpha_1 \mathbb{T} + \alpha_2 \mathbb{T}^2,$$

where $\mathbb{B} =_{\mathrm{def}} \mathbb{F}\mathbb{F}^\top$ denotes the left Cauchy–Green tensor, and $\{\alpha_i\}_{i=0}^2$ are scalar functions of mutually independent invariants of the Cauchy stress tensor $\mathbb{T}$ such as $\mathrm{Tr}\,\mathbb{T}$, $\mathrm{Tr}\,\mathbb{T}^2$ and $\mathrm{Tr}\,\mathbb{T}^3$.

A notable feature of models of type (1.1) is that they provide an elegant way to justify models wherein the *linearized* strain[1] $\mathbb{\varepsilon}$ is a *nonlinear* function of the stress, see for example Rajagopal [2, 5] for details. Indeed, in the small strain range the constitutive relation (1.1) can be linearized as

$$(1.2) \qquad \mathbb{\varepsilon} = \beta_0 \mathbb{I} + \beta_1 \mathbb{T} + \beta_2 \mathbb{T}^2.$$

The fact that one can appeal to the *linearization* with respect to the kinematical variables and yet consider *nonlinear response* of the material can not be overemphasised. Actually, the response of many materials is nonlinear even in the small strain range. For example, the response of portland-cement is nonlinear even if the displacement gradients are in the range where the linearized strain is definitely a fully acceptable approximation, see Grasley *et al.* [6] where the non-linear relation $\mathbb{\varepsilon} = \gamma_1(\mathrm{Tr}\,\mathbb{T})\mathbb{I} + \sinh[(\mathrm{Tr}\,\mathbb{T})^{\gamma_2}/\gamma_3]\mathbb{I} + \gamma_4\mathbb{T}$ is used to fit experimental data. The same observation holds for modern metallic alloys such as gum metal, see Saito *et al.* [7] and Kuramoto *et al.* [8], and other metallic alloys, see references in Bustamante and Rajagopal [9]. The experimental results of Saito *et al.* [7] have been correlated by Rajagopal [5] using the non-linear relation $\mathbb{\varepsilon} = \lambda_1(\mathrm{Tr}\,\mathbb{T})\mathbb{I} + 2\lambda_2 \mathrm{e}^{\eta\,\mathrm{Tr}\,\mathbb{T}}\mathbb{T}$. Thus, clearly for many materials the linearized elastic approximation cannot be used to correlate experimental data.

Since some materials exhibit nonlinear behaviour in the small strain range, using the classical linearized elastic response could lead to a miscalculation of the stresses even in the small strain regime. This error in the estimation of the stress can lead to serious errors in the estimation of the failure of structural members comprised of materials that exhibit such a nonlinear relationship between the strain and the stress. It is thus necessary to investigate carefully the response of structural members like beams, rods, plates and columns comprised of such materials, since an accurate analysis of their load bearing capacity is technologically important.

A simple but very useful and elegant beam theory is the classical Euler–Bernoulli beam theory, see for example Timoshenko and Goodier [10], which is yet widely used. This type of beam theory provides an excellent balance between mathematical complexity and accuracy of the descripiton of the behaviour

---

[1]Recall that $\mathbb{B} \approx \mathbb{I} + 2\mathbb{\varepsilon}$.

of the given structural element in a complex structural system. In what follows, we investigate the quantitative behaviour of nonlinear models of type (1.2) within the Euler–Bernoulli type setting.

We study the behaviour of a beam with fixed ends that is subject to uniform load or to a concentrated load in the middle of the beam. We derive a counterpart of the classical fourth order ordinary differential equation for the deflection of the beam. Unlike in the classical setting, see (2.20), the governing equations for the nonlinear material are given as a system of integro-differential equations, see (2.23). We solve the resulting system of integro-differential equations using a variant of the spectral collocation method. Quantitative differences between the stress and the deformation field for linear and nonlinear constitutive relation are discussed in the case of the quantitative material parameters that correspond to the data in Saito *et al.* [7] and Grasley *et al.* [6].

2. Euler–Bernoulli type beam theory

Let us briefly recall the classical derivation of the Euler–Bernoulli type beam theory. The aim is to clearly indicate the assumptions that are related to the assumed geometry of the motion and the assumptions concerning the constitutive relation for the given material.

Most of the assumptions that lead to the classical Euler–Bernoulli beam theory are the assumptions regarding the motion of the beam. As such, these assumptions are independent of the material model under consideration. This observation is essential in formulating beam theory for implicitly constituted materials of type (1.2) or other materials generalising the standard linearized elastic solid.

Following the classical approach, we consider the problem of small deflections of a beam of length $2L$ that is subjected to lateral loads only (see Fig. 1).
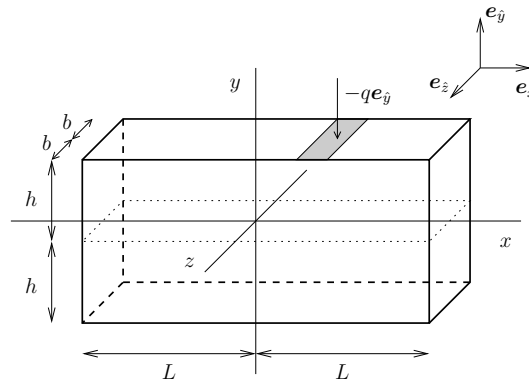

Fig. 1. Geometry of the beam.

For simplicity, we assume that the beam has a rectangular cross-section, and that the load on the upper surface is given in terms of its surface density q. Thus, the corresponding traction boundary condition on the upper surface reads $\mathbb{T}\boldsymbol{e}_{\hat{y}}|_{y=h} = -q\boldsymbol{e}_{\hat{y}}$. Other surfaces are assumed to be traction free.

2.1. Stress field

The stress field in the beam is assumed, as in the classical setting, to have the plane stress structure. Therefore, the *ansatz* for the stress tensor reads

$$(2.1) \qquad \mathbb{T} = \begin{bmatrix} \mathrm{T}_{\hat{x}\hat{x}} & \mathrm{T}_{\hat{x}\hat{y}} & 0 \\ \mathrm{T}_{\hat{x}\hat{y}} & \mathrm{T}_{\hat{y}\hat{y}} & 0 \\ 0 & 0 & 0 \end{bmatrix},$$

where $\mathrm{T}_{\hat{x}\hat{x}}$, $\mathrm{T}_{\hat{x}\hat{y}}$ and $\mathrm{T}_{\hat{y}\hat{y}}$ are functions of y and x only. If the stress field is given by (2.1), then the standard equilibrium equations in the absence of body forces, $\mathrm{div}\,\mathbb{T} = \mathbf{0}$, yield the following two nontrivial equations for the stress field,

$$(2.2a) \qquad \frac{\partial \mathrm{T}_{\hat{x}\hat{x}}}{\partial x} + \frac{\partial \mathrm{T}_{\hat{x}\hat{y}}}{\partial y} = 0,$$

$$(2.2b) \qquad \frac{\partial \mathrm{T}_{\hat{x}\hat{y}}}{\partial x} + \frac{\partial \mathrm{T}_{\hat{y}\hat{y}}}{\partial y} = 0.$$

Integrating the last equation with respect to y and z variables yields the relation between the averaged shear stress V (shearing force), $V =_{\mathrm{def}} \int_{y=-h}^{h} \mathrm{T}_{\hat{x}\hat{y}}\,dy$, and the load q,

$$(2.3) \qquad \frac{dV}{dx} - q = 0.$$

Indeed,

$$(2.4) \qquad 0 = \int\limits_{z=-b}^{b} \int\limits_{y=-h}^{h} \frac{\partial \mathrm{T}_{\hat{x}\hat{y}}}{\partial x}\,dy\,dz + \int\limits_{z=-b}^{b} \int\limits_{y=-h}^{h} \frac{\partial \mathrm{T}_{\hat{y}\hat{y}}}{\partial y}\,dy\,dz$$

$$= 2b\frac{d}{dx} \int\limits_{y=-h}^{h} \mathrm{T}_{\hat{x}\hat{y}}\,dy + 2b\left(\mathrm{T}_{\hat{y}\hat{y}}|_{y=h} - \mathrm{T}_{\hat{y}\hat{y}}|_{y=-h}\right) = 2b\frac{d}{dx}V - 2bq,$$

where we have used the boundary condition on the top and the bottom surface.

Further, multiplication of (2.2a) by y and subsequent integration with respect to y and z variables yields

$$(2.5) \qquad 0 = \int\limits_{z=-b}^{b} \int\limits_{y=-h}^{h} y \frac{\partial \mathrm{T}_{\hat{x}\hat{x}}}{\partial x} \, dy dz + \int\limits_{z=-b}^{b} \int\limits_{y=-h}^{h} y \frac{\partial \mathrm{T}_{\hat{x}\hat{y}}}{\partial y} \, dy dz$$

$$= 2b \frac{d}{dx} \int\limits_{y=-h}^{h} y \mathrm{T}_{\hat{x}\hat{x}} \, dy + 2b \int\limits_{y=-h}^{h} \frac{\partial}{\partial y} \left(y \mathrm{T}_{\hat{x}\hat{y}} \right) \, dy - 2b \int\limits_{y=-h}^{h} \mathrm{T}_{\hat{x}\hat{y}} \, dy$$

$$= 2b \frac{dM}{dx} + 2bh \left(\mathrm{T}_{\hat{x}\hat{y}}|_{y=h} + \mathrm{T}_{\hat{x}\hat{y}}|_{y=-h} \right) - 2bV = 2b \left(\frac{dM}{dx} - V \right),$$

where we have used the fact that the shear stress vanishes on the top and bottom surface, and where we have introduced the averaged z component of the bending moment M, $M =_{\mathrm{def}} \int_{y=-h}^{h} y \mathrm{T}_{\hat{x}\hat{x}} \, dy$.

We can therefore conclude that the following well known set of equations, see for example TIMOSHENKO and GERE [11],

$$(2.6\mathrm{a}) \qquad\qquad \frac{dV}{dx} - q = 0,$$

$$(2.6\mathrm{b}) \qquad\qquad \frac{dM}{dx} - V = 0,$$

follows exclusively from the assumption on the form of the stress field, see (2.1), and the imposed boundary conditions. Differentiating (2.6b) with respect to x and using (2.6a) one finally arrives at a single equation

$$(2.7) \qquad\qquad \frac{d^2 M}{dx^2} = q.$$

Note that the equations can be also derived by appealing to the balance of forces for an infinitesimal volume of the material, see for example TIMOSHENKO and GERE [11]. The expression for the relation between the bending moment and curvature must be however rederived for the nonlinear models. See for example SRINIVASA [12] for a discussion of the bending moment-curvature relations for incompressible solids that exhibit nonlinear response in the small strain range.

2.2. Strain field

The deformation of the beam is assumed to have the standard special form, see for example TIMOSHENKO and GERE [10]. The plane sections perpendicular to the midplane are assumed to remain plane sections perpendicular to the deformed midplane, see Fig. 2. Further, it is assumed that the position of the midplane is given by the function w. In such a case the point $[X, Y]$ in the reference configuration is moved to point $[x, y]$ in the current configuration, and the
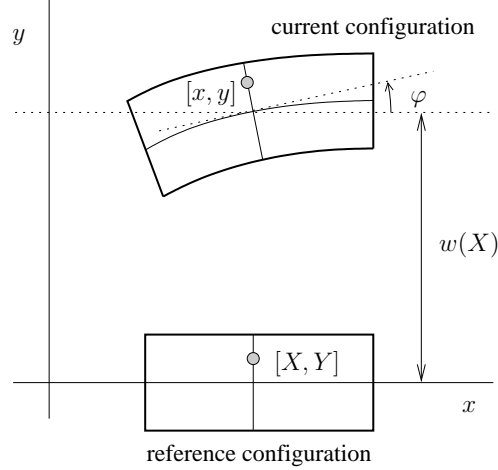
FIG. 2. Deflection of the beam.

formula for the deformation $\boldsymbol{\chi}$ reads

$$(2.8) \qquad \boldsymbol{x} = \boldsymbol{\chi}(\boldsymbol{X}) = \begin{bmatrix} X - Y\sin\varphi \\ w(X) + Y\cos\varphi \end{bmatrix},$$

where φ is the angle between the tangent to the deformed midplane and the horizontal axis. Consequently, the the displacement $\boldsymbol{u}(\boldsymbol{X}) =_{\text{def}} \boldsymbol{\chi}(\boldsymbol{X}) - \boldsymbol{X}$ is given by

$$(2.9) \qquad \boldsymbol{u}(\boldsymbol{X}) = \begin{bmatrix} -Y\sin\varphi \\ w(X) + Y(\cos\varphi - 1) \end{bmatrix},$$

and thus is the linearized strain tensor $\mathbb{e} =_{\text{def}} \frac{1}{2}(\nabla\boldsymbol{u} + (\nabla\boldsymbol{u})^\top)$, is given by the formula

$$(2.10) \qquad \mathbb{e} = \begin{bmatrix} -Y\cos\varphi\frac{d\varphi}{dX} & \frac{1}{2}\left(\frac{dw}{dX} - \sin\varphi - Y\sin\varphi\frac{d\varphi}{dX}\right) \\ \frac{1}{2}\left(\frac{dw}{dX} - \sin\varphi - Y\sin\varphi\frac{d\varphi}{dX}\right) & \cos\varphi - 1 \end{bmatrix}.$$

The derivative of the function w determines the angle φ between the tangent to the deformed midplane and the horizontal axis, $\tan\varphi = \frac{dw}{dX}$ (see Fig. 2). If we take into account the fact that the spatial variation of the deflection is assumed to be small, then we can write $\varphi \approx \sin\varphi$, $\tan\varphi \approx \varphi$ and $\cos\varphi \approx 1$. Using these formulae the displacement $\boldsymbol{u}$ can be approximated as

$$(2.11) \qquad \boldsymbol{u}(\boldsymbol{X}) = \begin{bmatrix} -Y\frac{dw}{dX} \\ w(X) \end{bmatrix}.$$

Further, the approximation of the small strain tensor ε reads

$$(2.12) \qquad \varepsilon = \begin{bmatrix} -Y\frac{d^2w}{dX^2} & 0 & 0 \\ 0 & 0 & 0 \\ 0 & 0 & 0 \end{bmatrix}.$$

Since we are dealing with small strain theory, we can ignore the difference between the reference and current configuration, abuse the notation and write

$$(2.13) \qquad \varepsilon = \begin{bmatrix} -y\frac{d^2w}{dx^2} & 0 & 0 \\ 0 & 0 & 0 \\ 0 & 0 & 0 \end{bmatrix}.$$

The assumptions concerning the kinematics are independent of the form of the constitutive relation for the material under consideration.

2.3. Constitutive relations

2.3.1. Classical linearized elastic solid. In the standard setting the material of the beam is assumed to be a linear, homogeneous and isotropic material, hence the relation between the Cauchy stress tensor $\mathbb{T}$ and linearized strain tensor ε reads

$$(2.14) \qquad \mathbb{T} = \lambda(\mathrm{Tr}\,\varepsilon)\mathbb{I} + 2\mu\varepsilon,$$

where the constants λ and μ are the Lamé parameters. Standard manipulation allows one to invert the constitutive relation (2.14) to arrive at

$$\varepsilon = \frac{1}{2\mu}\left(\mathbb{T} - \frac{\lambda}{3\lambda + 2\mu}(\mathrm{Tr}\,\mathbb{T})\mathbb{I}\right),$$

and get the following formulae for the strain components in the case of plane stress (2.1),

$$(2.15\mathrm{a}) \qquad \varepsilon_{\hat{x}\hat{x}} = \frac{\lambda + \mu}{\mu(3\lambda + 2\mu)}\left(\mathrm{T}_{\hat{x}\hat{x}} - \frac{\lambda}{2(\lambda + \mu)}\mathrm{T}_{\hat{y}\hat{y}}\right),$$

$$(2.15\mathrm{b}) \qquad \varepsilon_{\hat{y}\hat{y}} = \frac{\lambda + \mu}{\mu(3\lambda + 2\mu)}\left(\mathrm{T}_{\hat{y}\hat{y}} - \frac{\lambda}{2(\lambda + \mu)}\mathrm{T}_{\hat{x}\hat{x}}\right),$$

$$(2.15\mathrm{c}) \qquad \varepsilon_{\hat{x}\hat{y}} = \frac{1}{2\mu}\mathrm{T}_{\hat{x}\hat{y}},$$

while the other strain components vanish. Consequently, the *ansatz* for the strain field, which among others requires $\varepsilon_{\hat{y}\hat{y}} = 0$, is not consistent with the consequences for the strain from the *ansatz* for the stress field. However, this inconsistency in the classical approach is interpreted as negligible, and stress–strain

relation (2.15) is usually simplified to[2]

$$(2.16) \qquad \varepsilon_{\hat{x}\hat{x}} = \frac{1}{\mathrm{E}}\mathrm{T}_{\hat{x}\hat{x}},$$

and $\varepsilon_{\hat{y}\hat{y}} = 0$, $\varepsilon_{\hat{x}\hat{y}} = 0$, where we have further neglected $\mathrm{T}_{\hat{y}\hat{y}}$ component of the stress in (2.15a).

The reduction of a three-dimensional constitutive relation to a single relation between $\mathrm{T}_{\hat{x}\hat{x}}$ and $\varepsilon_{\hat{x}\hat{x}}$ that has been outlined above for a linearized material can also be applied in the case of more complex (nonlinear) constitutive relations.

2.3.2. Elastic solids with nonlinear constitutive relation in the small strain range. Concerning materials with nonlinear response in the linearized strain range Rajagopal [5] has considered constitutive relations

$$(2.17a) \qquad \varepsilon = \lambda_1(\mathrm{Tr}\,\mathbb{T})\mathbb{I} + 2\lambda_2 e^{\eta\,\mathrm{Tr}\,\mathbb{T}}\mathbb{T},$$

$$(2.17b) \qquad \varepsilon = \lambda_1(\mathrm{Tr}\,\mathbb{T})\mathbb{I} + \lambda_2(1 + \alpha\,|\mathbb{T}|^2)^n\mathbb{T},$$

where λ_1 is a negative constant, λ_2, η and α are positive constants, n is a constant and parameters λ_1, λ_2 must satisfy inequality $3\lambda_1 + 2\lambda_2 > 0$. The model introduced by Grasley *et al.* [6] reads

$$(2.17c) \qquad \varepsilon = \gamma_1(\mathrm{Tr}\,\mathbb{T})\mathbb{I} + \sinh[(\mathrm{Tr}\,\mathbb{T})^{\gamma_2}/\gamma_3]\mathbb{I} + \gamma_4\mathbb{T},$$

where γ_i are positive constants. Applying the approach discussed above, we see that the one-dimensional counterparts of three dimensional constitutive relations (2.17a)–(2.17c) are relations

$$(2.18a) \qquad \varepsilon_{\hat{x}\hat{x}} = (\lambda_1 + 2\lambda_2 e^{\eta\mathrm{T}_{\hat{x}\hat{x}}})\mathrm{T}_{\hat{x}\hat{x}},$$

$$(2.18b) \qquad \varepsilon_{\hat{x}\hat{x}} = (\lambda_1 + \lambda_2(1 + \alpha\mathrm{T}_{\hat{x}\hat{x}}^2)^n)\mathrm{T}_{\hat{x}\hat{x}},$$

$$(2.18c) \qquad \varepsilon_{\hat{x}\hat{x}} = \lambda_1\mathrm{T}_{\hat{x}\hat{x}} + \sinh(\mathrm{T}_{\hat{x}\hat{x}}^{\lambda_2}/\lambda_3).$$

(For the sake of consistency of the notation, we have relabeled the constants in (2.17c) as $\lambda_1 =_{\mathrm{def}} \gamma_1 + \gamma_4$, $\lambda_2 =_{\mathrm{def}} \gamma_2$ and $\lambda_3 =_{\mathrm{def}} \gamma_3$.)

2.4. Governing equations

2.4.1. Classical linearized elastic solid. In the case of the classical linearized elastic solid model (2.16), the generic equation (2.7) reduces in virtue of (2.13) to

$$(2.19) \qquad \frac{d^2}{dx^2}\left(-\int_{y=-h}^{h} y^2\mathrm{E}\frac{d^2w}{dx^2}\,dy\right) = q$$

---

[2]Recall that Young modulus and Poisson ratio are given by the formulae $\mathrm{E} =_{\mathrm{def}} \frac{\mu(3\lambda+2\mu)}{\lambda+\mu}$ and $\nu =_{\mathrm{def}} \frac{\lambda}{2(\lambda+\mu)}$.

which upon integration yields the classical fourth order linear ordinary differential equation

$$(2.20) \qquad \frac{d^2}{dx^2}\left(-\mathrm{E}I\frac{d^2w}{dx^2}\right) = q,$$

where I denotes the second moment of the cross-section of the beam, $I =_{\mathrm{def}} \int_{y=-h}^{h} y^2\,dy = \frac{2h^3}{3}$.

2.4.2. Elastic solids with nonlinear constitutive relation in the small strain range
For a material with nonlinear response in the small strain range the generic equations (2.6) reduce to

$$(2.21) \qquad \frac{d^2M}{dx^2} = q.$$

Unlike in the classical case, the bending moment

$$M = \int\limits_{y=-h}^{h} y\mathrm{T}_{\hat{x}\hat{x}}\,dy$$

is not an explicit function of the deflection w of the beam. This is a consequence of the fact that the stress $\mathrm{T}_{\hat{x}\hat{x}}$ that needs to be substituted into the formula for the bending moment is not given as an explicit function of the strain or the second derivative of the deflection $\frac{d^2w}{dx^2}$ and y as in the classical case. Depending on the parameter values in (2.18), it could even happen that the constitutive relation of the type (2.18) is not invertible at all, meaning that it can not be rewritten in the form $\mathrm{T}_{\hat{x}\hat{x}} = h(\varepsilon_{\hat{x}\hat{x}})$.

In the parameter range that is studied below, we deal with the constitutive relations of the form $\varepsilon_{\hat{x}\hat{x}} = g(\mathrm{T}_{\hat{x}\hat{x}})$ that are formally invertible, but it is inconvenient or impractical to invert the constitutive relation in order to get $\mathrm{T}_{\hat{x}\hat{x}}$ as a function of $\frac{d^2w}{dx^2}$ and y. The reason is that the inverse relation can not be, except of some special cases[3], easily expressed by a simple analytical formula. Consequently, the counterpart of the classical equation (2.20) for model (2.18a) is the

---

[3]For example, setting $\lambda_1 = 0$ in the constitutive relation (2.18a), one can find an explicit relation for $\mathrm{T}_{\hat{x}\hat{x}}$ as a function of $\varepsilon_{\hat{x}\hat{x}} = -y\frac{d^2w}{dx^2}$. Indeed, using the Lambert W function one can write $\mathrm{T}_{\hat{x}\hat{x}}(x,y) = \frac{1}{\eta}\mathrm{W}\left(-\frac{\eta}{2\lambda_2}\frac{d^2w}{dx^2}y\right)$, and substitute this formula into the equation for the bending moment $\frac{d^2}{dx^2}\left(\int_{y=-h}^{h} y\mathrm{T}_{\hat{x}\hat{x}}\,dy\right) = q$. In such a case the final governing equation reads

$$(2.22) \qquad \frac{d^2}{dx^2}\left(\frac{1}{\eta}\int\limits_{y=-h}^{h} y\mathrm{W}\left(-\frac{\eta}{2\lambda_2}\frac{d^2w}{dx^2}y\right)\,dy\right) = q,$$

which is clearly a counterpart of the classical equation (2.19).

following system of equations for the deflection $w(x)$ and the stress field $\mathrm{T}_{\hat{x}\hat{x}}(x, y)$

(2.23a) $$\frac{d^2}{dx^2}\left(\int\limits_{y=-h}^{h} y\mathrm{T}_{\hat{x}\hat{x}}\, dy \right) = q,$$

(2.23b) $$y\frac{d^2w}{dx^2} = -(\lambda_1 + 2\lambda_2 \mathrm{e}^{\eta\mathrm{T}_{\hat{x}\hat{x}}})\mathrm{T}_{\hat{x}\hat{x}},$$

and similarly for other models of type (2.18).

The governing equations for the materials with nonlinear response in the small strain range are therefore integro–differential equations which need to be solved simultaneously. Also note that (2.23) is a system of lower order equations rather than the fourth order equation (2.20) which might also have implications for the boundary conditions as it is not necessary to prescribe the boundary conditions purely for the deflection w anymore.

2.5. Boundary conditions

Besides the governing equations, it is necessary to specify the boundary conditions. The specification of the boundary conditions is straightforward if we consider fixed ends. This boundary condition is a kinematical one, and does not depend on a particular constitutive relation for the material of the beam. The boundary conditions for the fixed ends of the beam of length $2L$ (see Fig. 1), read

(2.24a) $$w|_{x=\pm L} = 0,$$

(2.24b) $$\frac{dw}{dx}\bigg|_{x=\pm L} = 0.$$

Concerning the other possible boundary conditions that involve shearing force V and/or bending moment M, the specification of the boundary conditions is more complicated. It is clear that if one wants to rewrite boundary conditions that contain V or M in terms of deflection w, then the boundary conditions will be model dependent. (The relation between the stress and w depends on the constitutive relation.) In particular, we must take this observation into account when we try to exploit the symmetry of the problem using the slider (roller) boundary condition.

The beam is assumed to be homogeneous, isotropic and of constant cross-section, hence it is symmetric with respect to the origin of the chosen coordinate system. Moreover, the considered loads (uniform load, concentrated load at origin) are also symmetric. The symmetry of the problem can be exploited in the numerical solution. The computational domain can be effectively restricted to

$[0, L]$ provided that we supply the governing equations with artificial boundary conditions enforcing the symmetry of the solution at $x = 0$.

The symmetry of the solution can be enforced by the sliding (roller) boundary condition at the axis of symmetry $x = 0$, see HAN *et al.* [13]. This condition allows the center of the beam to move freely in the vertical direction, and it prevents the cross-section from rotating. In mathematical terms, the conditions for the artificial sliding end read

$$(2.25a) \qquad \left.\frac{dw}{dx}\right|_{x=0} = 0,$$

$$(2.25b) \qquad V(0) = \left.\frac{dM}{dx}\right|_{x=0} = 0,$$

where we have used relation (2.6b).

For the classical linearized elastic solid the boundary condition (2.25b) reduces – in virtue of the constitutive relation (2.16) and strain-deflection relation (2.13) – to

$$(2.26) \qquad V(0) = \left.\frac{dM}{dx}\right|_{x=0} = \left[\frac{d}{dx}\left(\int_{y=-h}^{h} y\mathrm{T}_{\hat{x}\hat{x}}\, dy\right)\right]\Bigg|_{x=0}$$

$$= -\mathrm{E}I\left.\frac{d^3w}{dx^3}\right|_{x=0} = 0.$$

Since $\mathrm{E}I$ is a constant, the last equation reduces to $\frac{d^3w}{dx^3}\big|_{x=0} = 0$, which is the classical form of the sliding boundary condition.

If we consider materials with nonlinear response of type (2.18) where the stress is not necessarily given as an explicit function of the strain, then it is impractical or impossible to substitute for $\mathrm{T}_{\hat{x}\hat{x}}$ in (2.25b), and reduce the boundary condition to a single condition for the derivatives of w as in the classical setting. Therefore, boundary condition (2.25b) is left in the form

$$(2.27) \qquad \left[\frac{d}{dx}\left(\int_{y=-h}^{h} y\mathrm{T}_{\hat{x}\hat{x}}\, dy\right)\right]\Bigg|_{x=0} = 0.$$

2.6. Load

We shall consider two kinds of lateral loads acting on the beam, namely a uniform load and a concentrated load. In case of the uniform load (see Fig. 3a), we have
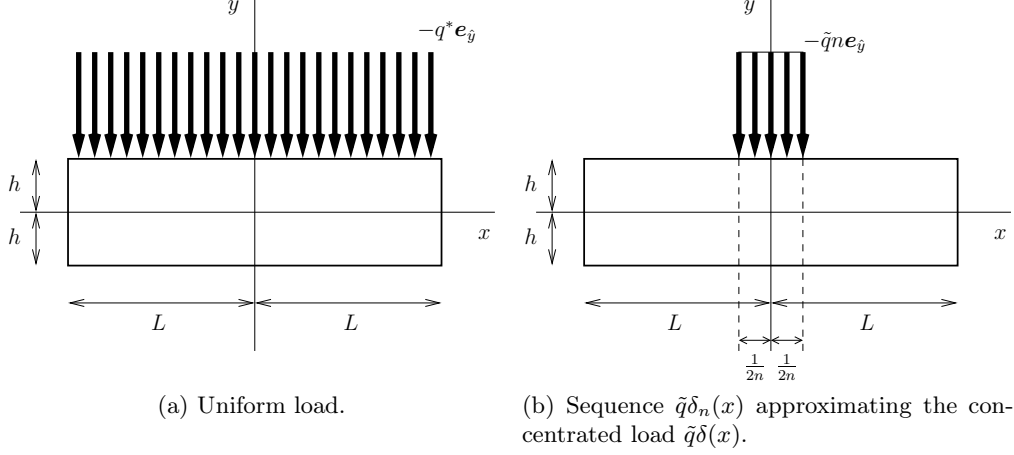
(a) Uniform load.

(b) Sequence $\tilde{q}\delta_n(x)$ approximating the concentrated load $\tilde{q}\delta(x)$.

FIG. 3. Lateral loads acting on the beam.

$$(2.28) \qquad\qquad q(x) = q^*,$$

where q^* is a positive constant. Concerning the concentrated load, we assume a pointwise load $\tilde{q}$ at the origin, that is

$$(2.29) \qquad\qquad q(x) = \tilde{q}\delta(x),$$

where $\delta(\cdot)$ is the Dirac distribution and $\tilde{q}$ is, once again, some positive constant.

Since we want to exploit the symmetry of the problem and solve the governing equations in $[0, L]$, we must be careful in handling the problem with the concentrated load at $x = 0$. If the load is *concentrated* at $x = 0$, we have to adjust the artificial sliding end boundary condition (2.25b) in an appropriate way.

The specification of the boundary condition for the concentrated load is based on the following calculation. First, the concentrated load can be interpreted as a limit of a sequence of spatially distributed loads

$$(2.30) \qquad \tilde{q}\delta_n(x) = \begin{cases} 0 & x < -\frac{1}{2n}, \\ \tilde{q}n & -\frac{1}{2n} \le x \le \frac{1}{2n}, \\ 0, & \frac{1}{2n} < x, \end{cases}$$

see Fig. 3b. The governing equations for the spatially distributed load are (2.23), and the artificial sliding end boundary condition is (2.27). Integrating (2.23) from $x = 0$ to $x = \frac{1}{2n}$ yields

$$(2.31) \qquad \int\limits_{x=0}^{1/(2n)} \left(\frac{d^2}{dx^2} \left(\int\limits_{y=-h}^{h} y \mathrm{T}_{\hat{x}\hat{x}}(x, y)\, dy \right) \right) dx = \int\limits_{x=0}^{1/(2n)} \tilde{q}\delta_n(x)\, dx.$$

Using the boundary condition (2.27) then leads to

$$(2.32) \qquad \left[\frac{d}{dx} \left(\int_{y=-h}^{h} y \mathrm{T}_{\hat{x}\hat{x}}(x,y)\, dy \right) \right]\Bigg|_{x=\frac{1}{2n}} - \left[\frac{d}{dx} \left(\int_{y=-h}^{h} y \mathrm{T}_{\hat{x}\hat{x}}(x,y)\, dy \right) \right]\Bigg|_{x=0}$$

$$= \left[\frac{d}{dx} \left(\int_{y=-h}^{h} y \mathrm{T}_{\hat{x}\hat{x}}(x,y)\, dy \right) \right]\Bigg|_{x=\frac{1}{2n}},$$

hence (2.31) reduces to

$$(2.33) \qquad \left[\frac{d}{dx} \left(\int_{y=-h}^{h} y \mathrm{T}_{\hat{x}\hat{x}}(x,y)\, dy \right) \right]\Bigg|_{x=1/(2n)} = \frac{\tilde{q}}{2}.$$

Taking the limit $n \to +\infty$ in (2.33) yields the effective boundary condition for the concentrated load,

$$(2.34) \qquad \left[\frac{d}{dx} \left(\int_{y=-h}^{h} y \mathrm{T}_{\hat{x}\hat{x}}(x,y)\, dy \right) \right]\Bigg|_{x=0} = \frac{\tilde{q}}{2}.$$

The governing equation for the concentrated load then reads simply

$$(2.35) \qquad \frac{d^2}{dx^2} \left(\int_{y=-h}^{h} y \mathrm{T}_{\hat{x}\hat{x}}(x,y)\, dy \right) = 0.$$

(Clearly, the concentrated load is not located in the interval $(0, L)$. This can be again seen by interpreting the concentrated load as a limit of spatially distributed loads.)

3. Numerical solution

3.1. System of governing equations

The final system of governing equations and boundary conditions for the deflection $w(x)$, $w : [0, L] \mapsto \mathbb{R}$ and the stress field $\mathrm{T}_{\hat{x}\hat{x}}(x,y)$, $\mathrm{T}_{\hat{x}\hat{x}} : [0, L] \times [-h, h] \mapsto \mathbb{R}$ of a beam made of material (2.18a) under the uniform load reads

$$(3.1a) \qquad \frac{d^2}{dx^2} \left(\int_{y=-h}^{h} y \mathrm{T}_{\hat{x}\hat{x}}\, dy \right) = q^*,$$

$$(3.1b) \qquad y \frac{d^2 w}{dx^2} = -(\lambda_1 + 2\lambda_2 e^{\eta \mathrm{T}_{\hat{x}\hat{x}}}) \mathrm{T}_{\hat{x}\hat{x}},$$

$$(3.1\text{c}) \qquad\qquad\qquad\qquad w|_{x=L} = 0,$$

$$(3.1\text{d}) \qquad\qquad\qquad\qquad \left.\frac{dw}{dx}\right|_{x=L} = 0,$$

$$(3.1\text{e}) \qquad\qquad\qquad\qquad \left.\frac{dw}{dx}\right|_{x=0} = 0,$$

$$(3.1\text{f}) \qquad\qquad \frac{d}{dx}\left(\int_{y=-h}^{h} y\mathrm{T}_{\hat{x}\hat{x}}\,dy\right)\Bigg|_{x=0} = 0.$$

(Recall that the deflection of the whole beam $[-L, L]$ is obtained by symmetry.) If the beam is subject to the concentrated load at $x = 0$, then the right hand side of (3.1a) is equal to zero, and the boundary condition (3.1f) is replaced by (2.34). The equations for material with constitutive relation (2.18b), (2.18c) and (2.16) respectively differ only in the right hand side of (3.1b).

In the case of the uniform load and the classical linearized elastic solid with constitutive relation (2.16) the corresponding variant of system (3.1) can be solved analytically. The solution reads

$$(3.2) \qquad\qquad\qquad w(x) = -\frac{q^*(L^2 - x^2)^2}{16h^3\mathrm{E}},$$

and the corresponding stress distribution can be computed using the equation $\mathrm{T}_{\hat{x}\hat{x}}(x, y) = -\mathrm{E}y\frac{d^2w}{dx^2}$.

The analytical solution for the classical linearized solid in the case of the concentrated load is

$$(3.3) \qquad\qquad w(x) = -\frac{\tilde{q}}{16h^3\mathrm{E}}((L - 2x)(L + x)^2 + 4x^3H(x)),$$

where $H(\cdot)$ denotes the Heaviside function. These analytical solutions can be used for testing the numerical scheme and for comparison between the behaviour of the material with the classical linearized constitutive relation and its nonlinear counterparts.

3.2. Spectral collocation method

Concerning nonlinear materials, we solve the problem numerically using a variant of the spectral collocation method, see for example Trefethen [14]. The physical domain $[x, y] \in [0, L] \times [-h, h]$ is first transformed to the computational domain $[\tilde{x}, \tilde{y}] \in [-1, 1] \times [-1, 1]$ which is then discretised using a grid

based on Gauss–Lobatto–Chebyshev points

$$(3.4a) \qquad \tilde{x}_i = \cos\left(\frac{(i-1)\pi}{N-1}\right), \qquad i = 1, \ldots, N,$$

$$(3.4b) \qquad \tilde{y}_j = \cos\left(\frac{(j-1)\pi}{M-1}\right), \qquad j = 1, \ldots, M,$$

where N and M denote the number of collocation points in each direction. For differentiation, we use spectral differentiation matrices in the form given by WIDEMAN and REDDY [15], and for numerical evaluation of the integrals in (3.1a) and (3.1f), we use the Clenshaw–Curtis quadrature, see for example GENTLEMAN [16, 17], VON WINCKEL [18] and WALDVOGEL [19].

The full nonlinear system (3.1) is solved by the Newton–Raphson method with the Jacobian matrix being computed analytically. Equation (3.1a) is enforced in $N-4$ collocation points (ommiting two points at each boundary) and Eq. (3.1b) is enforced in all NM collocation points. Together with the boundary conditions, this results in a system of $N-1+NM$ equations for $N-1$ unknown values of the deflection[4] $w(x)$ at the collocation points and NM unknown values of the stress $\mathrm{T}_{\hat{x}\hat{x}}$ at the collocation points.

In all the numerical simulations reported below, we have used a grid of size $N = M = 32$.

4. Results

4.1. Parameter values

To determine the parameter values of the model (2.18a), we have fitted the data by SAITO *et al.* [7] (see Fig. 4). The corresponding parameter values are

$$(4.1) \qquad \begin{aligned} \lambda_1 &= -2.22 \times 10^{-8} \ \mathrm{MPa}^{-1}, \\ \lambda_2 &= 7.01 \times 10^{-6} \ \mathrm{MPa}^{-1}, \\ \eta &= 4.44 \times 10^{-4} \ \mathrm{MPa}^{-1}. \end{aligned}$$

Further, let us assume that the same data set is fitted using the classical linearized stress–strain relation (2.16). Taking the derivative of equation (2.18a) at $\mathrm{T}_{\hat{x}\hat{x}} = 0$ yields

$$(4.2) \qquad \left.\frac{\partial \varepsilon_{\hat{x}\hat{x}}}{\partial \mathrm{T}_{\hat{x}\hat{x}}}\right|_{\mathrm{T}_{\hat{x}\hat{x}}=0} = \lambda_1 + 2\lambda_2.$$

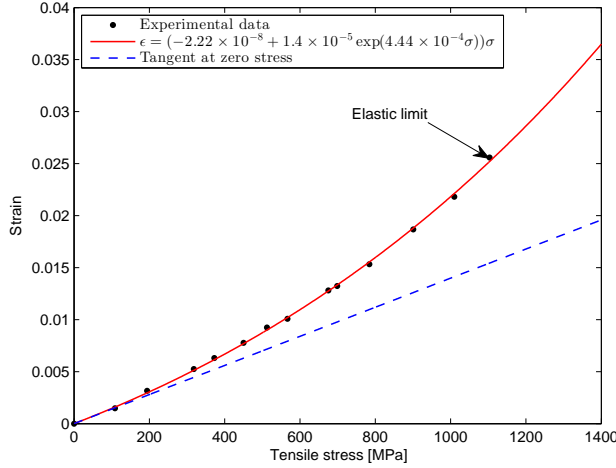[4]Recall that $w(L)$ is known. It is specified by the boundary condition.

Fig. 4. Constitutive relation for a gum metal alloy. Experimental data taken from Saito *et al.* [7].

Consequently, the Young modulus in (2.16) is related to the coefficients λ_1 and λ_2 in (2.18a) via the equality

$$(4.3) \qquad E = \frac{1}{\lambda_1 + 2\lambda_2},$$

and for the values listed in (4.1) we get

$$(4.4) \qquad E = 7.1 \times 10^4 \text{ MPa}.$$

Considering the model (2.18c), values of the phenomenological coefficients λ_i have been determined as the arithmetic mean of the corresponding coefficients for the axial strain response from Table 2 in Grasley *et al.* [6]. For simplicity, we assume $\lambda_2 \equiv 1$. (The actual value of the mean obtained from data by Grasley *et al.* [6] is 0.9.) The mean values of the remaining coefficients are

$$(4.5) \qquad \lambda_1 = 23.1 \times 10^{-6} \text{ MPa}^{-1}, \qquad \lambda_3 = 8.6 \text{ MPa}.$$

If the same data set is fitted using the standard linearized relation (2.16), then the value of the Young modulus is

$$(4.6) \qquad E = \frac{1}{\lambda_1} = 43.3 \text{ GPa}.$$

4.2. Comparison of the models.

Having the experimental data, one could opt for using a nonlinear stress–strain relation or the standard linearized stress–strain relation as a model for the material behaviour. Clearly, the standard linearized stress–strain relation provides a good approximation of the actual behaviour of the material only for extremely small strains (see for example Fig. 4). The question is whether using the classical linearized model instead of the actual nonlinear behaviour of the

(a) Deflection w^{LIN} predicted by the linear stress–strain relation (2.16).

(b) Stress field $\mathrm{T}_{\hat{x}\hat{x}}^{\mathrm{LIN}}$ predicted by the linear stress–strain relation (2.16).

(c) Difference $w^{\mathrm{LIN}} - w$ between the deflection w^{LIN} predicted by the linear stress–strain relation (2.16), and the deflection w predicted by the nonlinear stress–strain relation (2.18a).

(d) Difference $\mathrm{T}_{\hat{x}\hat{x}}^{\mathrm{LIN}} - \mathrm{T}_{\hat{x}\hat{x}}$ between the stress field $\mathrm{T}_{\hat{x}\hat{x}}^{\mathrm{LIN}}$ predicted by the linear stress–strain relation (2.16), and the stress field $\mathrm{T}_{\hat{x}\hat{x}}$ predicted by the nonlinear stress–strain relation (2.18a).
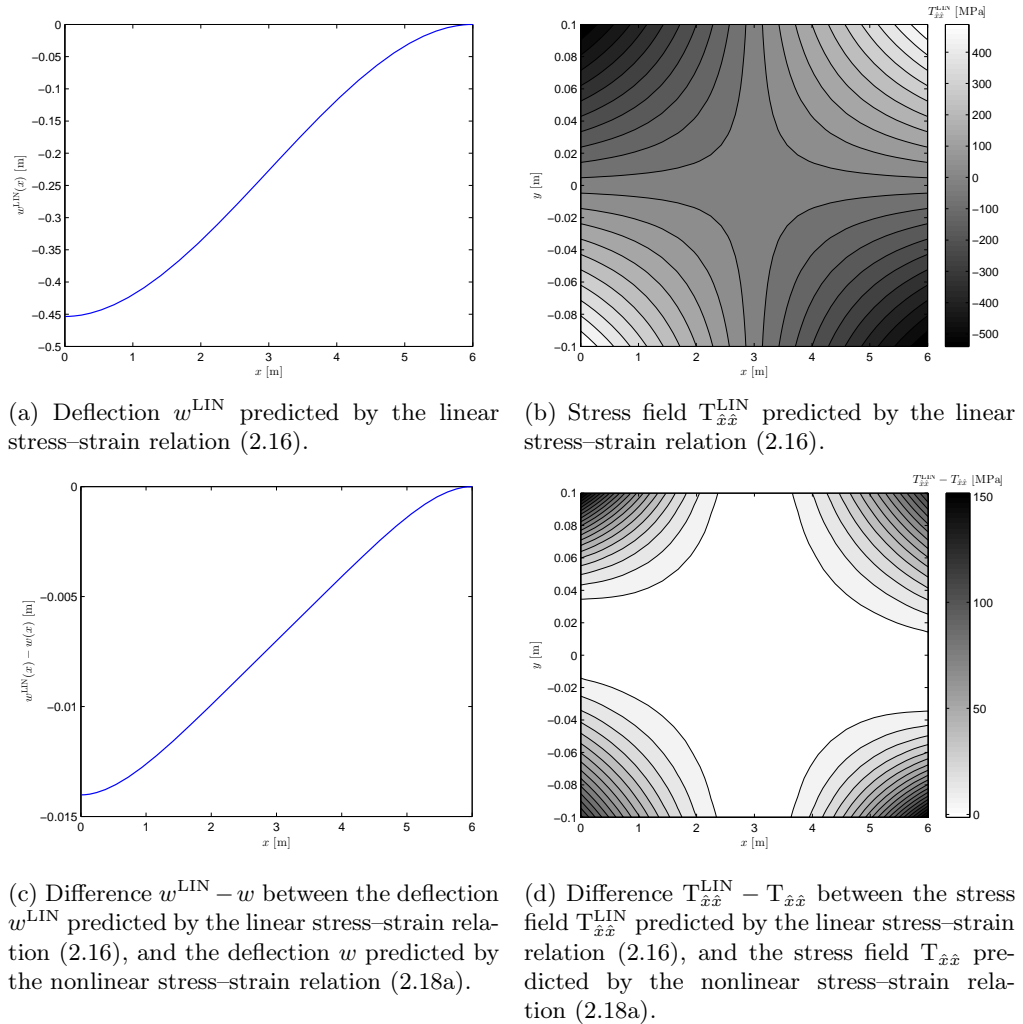
Fig. 5. Gum metal alloy. Comparison of the deflection and the stress field predicted by the linear model (2.16) and the nonlinear model (2.18a) under a concentrated load at $x = 0$. Parameter values are $L = 6$ m, $h = 0.1$ m, $\lambda_1 = -2.22 \times 10^{-8}$ MPa^{-1}, $\lambda_2 = 7.01 \times 10^{-6}$ MPa^{-1}, $\eta = 4.44 \times 10^{-4}$ MPa^{-1}, $\tilde{q} = 2.4$ MPa.

material has a significant quantitative impact on the predicted deflection and the stress distribution. In what follows, *we investigate the deflection and the stress distribution in a beam with fixed ends, and we compare the results based on the standard linearized stress–strain relation and on a nonlinear stress–strain relation.*

The results for the gum metal alloy are shown in Fig. 5 and 6. Here the nonlinear model used is the model (2.18a) with parameters given in (4.1). Figure 5 shows the deflection and the stress distribution in the beam under a concentrated load. The difference between the deflection predicted using the linearized

(a) Deflection w^{LIN} predicted by the linear stress–strain relation (2.16).

(b) Stress field $\mathrm{T}_{\hat{x}\hat{x}}^{\mathrm{LIN}}$ predicted by the linear stress–strain relation (2.16).

(c) Difference $w^{\mathrm{LIN}} - w$ between the deflection w^{LIN} predicted by the linear stress–strain relation (2.16), and the deflection w predicted by the nonlinear stress–strain relation (2.18a).

(d) Difference $\mathrm{T}_{\hat{x}\hat{x}}^{\mathrm{LIN}} - \mathrm{T}_{\hat{x}\hat{x}}$ between the stress field $\mathrm{T}_{\hat{x}\hat{x}}^{\mathrm{LIN}}$ predicted by the linear stress–strain relation (2.16), and the stress field $\mathrm{T}_{\hat{x}\hat{x}}$ predicted by the nonlinear stress–strain relation (2.18a).
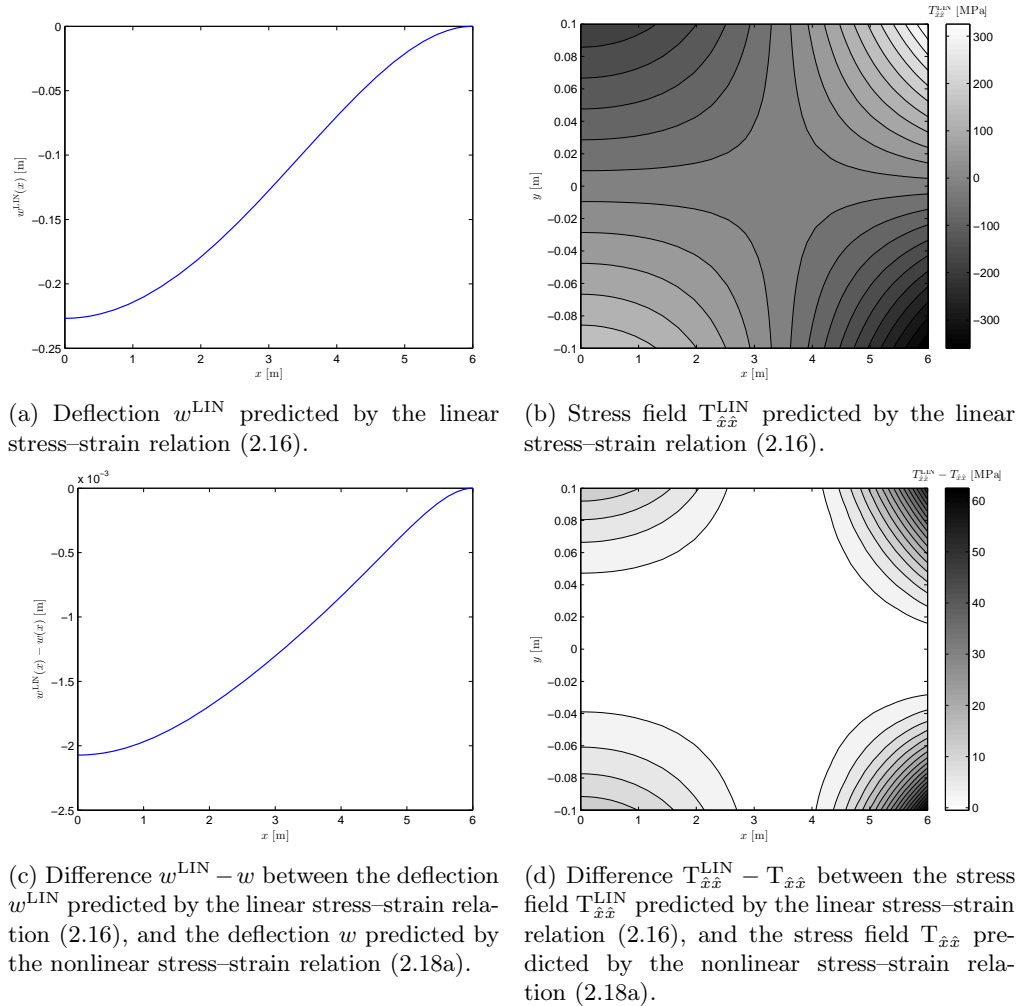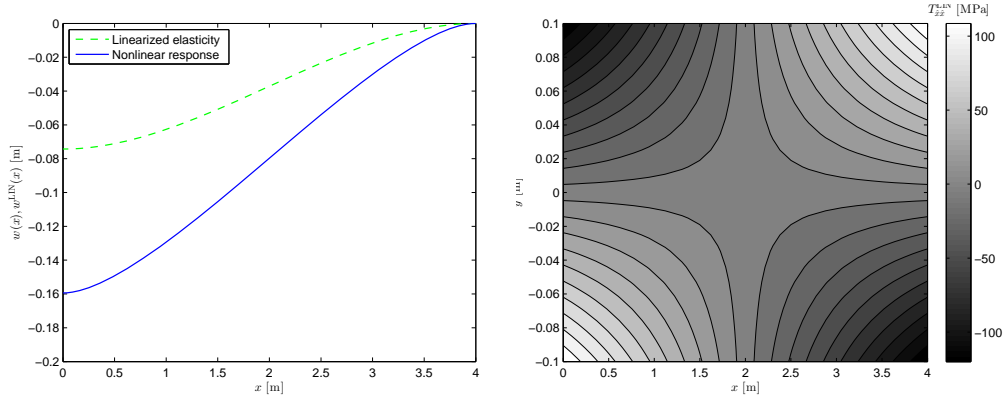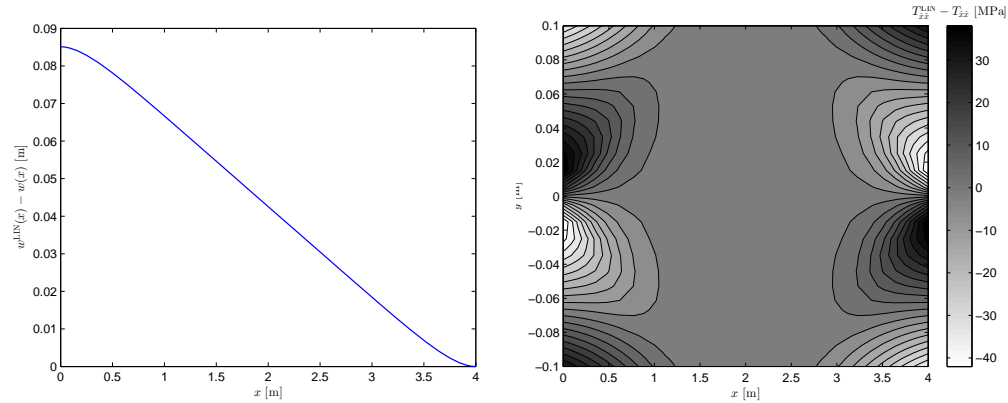
FIG. 6. Gum metal alloy. Comparison of the deflection and the stress field predicted by the linear model (2.16) and the nonlinear model (2.18a) under a uniform load. Parameter values are $L = 6$ m, $h = 0.1$ m, $\lambda_1 = -2.22 \times 10^{-8}$ MPa^{-1}, $\lambda_2 = 7.01 \times 10^{-6}$ MPa^{-1}, $\eta = 4.44 \times 10^{-4}$ MPa^{-1}, $q^* = 0.2$ MPa.

model and the nonlinear model is in the considered case of order 10^{-3} m which makes the difference negligible relative to the magnitude of the deflection that is of order 10^{-1} m (see Fig. 5a and 5c). On the other hand, the difference between the predicted stress field values $T_{\hat{x}\hat{x}}$ can be as high as 50 MPa, while the maximal magnitude of the stress field is around 500 MPa (see Fig. 5b and 5d). The

(a) Deflection w^{LIN} predicted by the linear stress–strain relation (2.16), and the deflection w predicted by the nonlinear stress–strain relation (2.18c).

(b) Stress field $T_{\hat{x}\hat{x}}^{\mathrm{LIN}}$ predicted by the linear stress–strain relation (2.16).

(c) Difference $w^{\mathrm{LIN}} - w$ between the deflection w^{LIN} predicted by the linear stress–strain relation (2.16), and the deflection w predicted by the nonlinear stress–strain relation (2.18c).

(d) Difference $T_{\hat{x}\hat{x}}^{\mathrm{LIN}} - T_{\hat{x}\hat{x}}$ between the stress field $T_{\hat{x}\hat{x}}^{\mathrm{LIN}}$ predicted by the linear stress–strain relation (2.16), and the stress field $T_{\hat{x}\hat{x}}$ predicted by the nonlinear stress–strain relation (2.18c).

FIG. 7. Portland-cement concrete. Comparison of the deflection and the stress field predicted by the linear model (2.16) and the nonlinear model (2.18c) under a concentrated load at $x = 0$. Parameter values are $L = 4$ m, $h = 0.1$ m, $\lambda_1 = 23.1 \times 10^{-6}$ MPa^{-1}, $\lambda_2 = 1$, $\lambda_3 = 8.6$ MPa, $\tilde{q} = 0.8$ MPa.

difference between the predicted stress fields is therefore of the order of tenths of percents which is a large difference. *Since failure is usually based on the values of stress, the difference in the maximum value of the stresses in the two cases can assume significance.*

The results for the uniform load are qualitatively the same as for the concentrated load (see Fig. 6). We can therefore conclude that in the studied settings
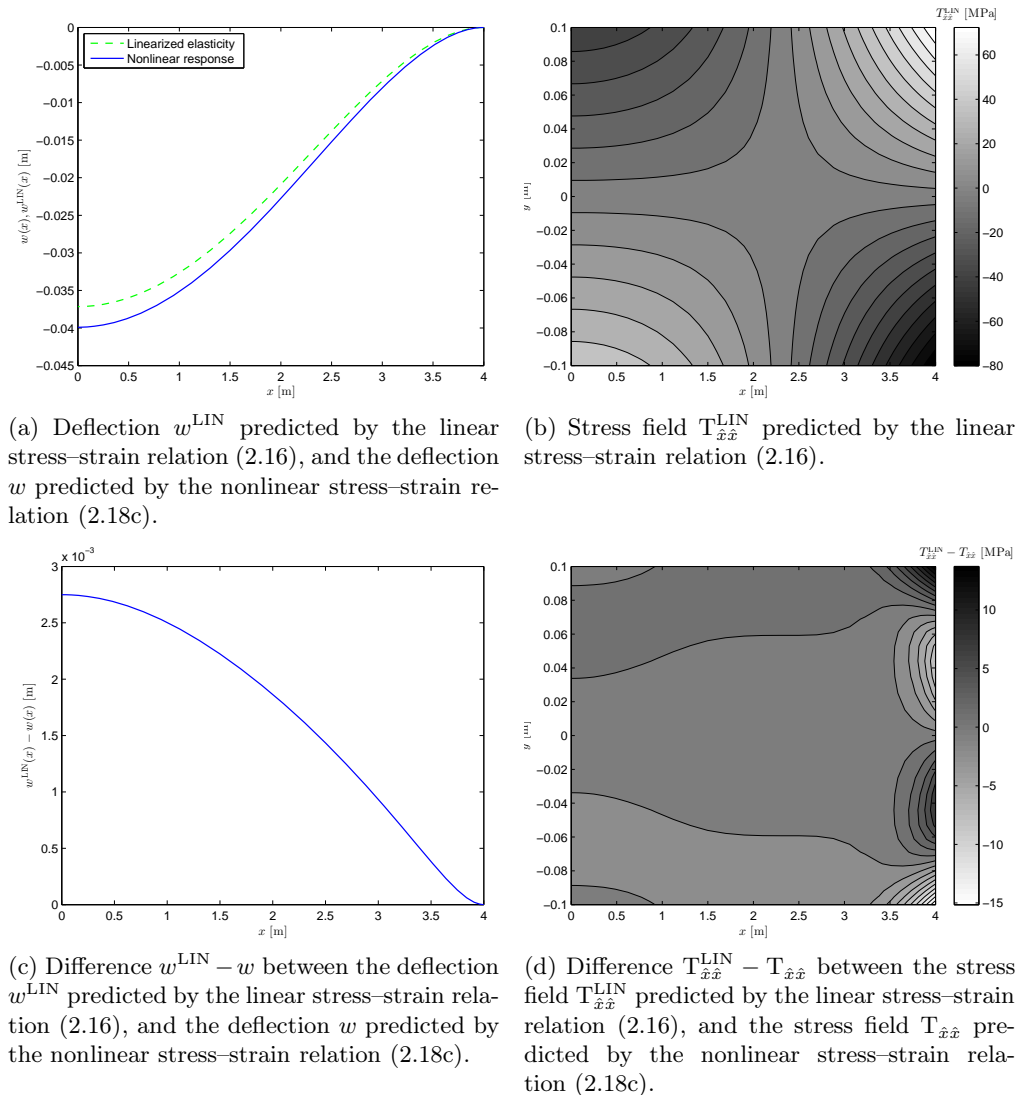

(a) Deflection w^{LIN} predicted by the linear stress–strain relation (2.16), and the deflection w predicted by the nonlinear stress–strain relation (2.18c).

(b) Stress field $\mathrm{T}^{\mathrm{LIN}}_{\hat{x}\hat{x}}$ predicted by the linear stress–strain relation (2.16).

(c) Difference $w^{\mathrm{LIN}} - w$ between the deflection w^{LIN} predicted by the linear stress–strain relation (2.16), and the deflection w predicted by the nonlinear stress–strain relation (2.18c).

(d) Difference $\mathrm{T}^{\mathrm{LIN}}_{\hat{x}\hat{x}} - \mathrm{T}_{\hat{x}\hat{x}}$ between the stress field $\mathrm{T}^{\mathrm{LIN}}_{\hat{x}\hat{x}}$ predicted by the linear stress–strain relation (2.16), and the stress field $\mathrm{T}_{\hat{x}\hat{x}}$ predicted by the nonlinear stress–strain relation (2.18c).

Fig. 8. Portland-cement concrete. Comparison of the deflection and the stress field predicted by the linear model (2.16) and the nonlinear model (2.18c) under a uniform load. Parameter values are $L = 4$ m, $h = 0.1$ m, $\lambda_1 = 23.1 \times 10^{-6}$ MPa^{-1}, $\lambda_2 = 1$, $\lambda_3 = 8.6$ MPa, $q^* = 0.1$ MPa.
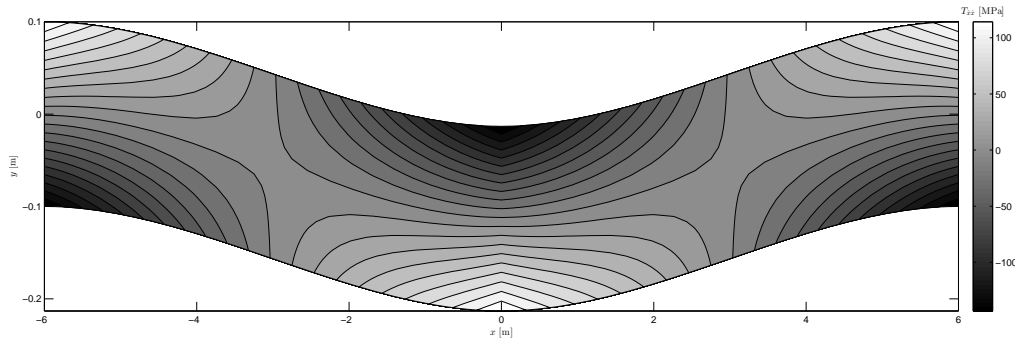
Fig. 9. Gum metal alloy. Stress field predicted by the nonlinear model (2.18a) under a concentrated load at $x = 0$ in the deformed domain. Parameter values are $L = 6$ m, $h = 0.1$ m, $\lambda_1 = -2.22 \times 10^{-8}$ MPa^{-1}, $\lambda_2 = 7.01 \times 10^{-6}$ MPa^{-1}, $\eta = 4.44 \times 10^{-4}$ MPa^{-1}, $\tilde{q} = 0.6$ MPa.

the chosen loading leads for the linearized and the nonlinear model to almost identical deflections, while the predicted stress fields are considerably different. This finding qualitatively corresponds to the results expected from the inspection of Fig. 4 that shows the results based on the one-dimensional nonlinear constitutive relation. Here we see that the identical strains generate different stresses depending on the choice of the model.

The overall view of the stress field in the deformed configuration is shown in Fig. 9.

The results for concrete are shown in Fig. 7 and 8. Here the nonlinear model is the model (2.18c) with parameters given in (4.5). In this case the nonlinearity of the material and the chosen load lead to a large discrepancy even for the *deflection* predicted on the basis of the linearized and the nonlinear model. Under concentrated load conditions, the maximal deflection predicted by the linear model is nearly half the deflection predicted by the nonlinear model (see Fig. 7a). Similar observations are valid also for the stress (see Fig. 7b and 7d). One should also notice that the spatial distribution of the difference between the stress field predicted by the linearized model and the nonlinear model is rather complex. Note that the difference between the predicted stress fields is not, unlike in the previous case (see Fig. 5d), concentrated in the corners (see Fig. 7d).

5. Conclusion

We have studied the deformation of beams made of materials with nonlinear constitutive relations in the small strain range. The deflection of the beams has been studied within the Euler–Bernoulli type setting that in the small strain

range provide a reasonable balance between the complexity of the mathematical description and the usability of the obtained results. We have formulated the problem of the deflection of the beams as a system of nonlinear integro-differential equations, and we have solved the system numerically using a variant of the spectral collocation method. The numerical results obtained for two particular nonlinear models that fit experimental data for gum metal and concrete have been compared to the results obtained by the corresponding linearized models.

The nonlinear models are the models that are more physically realistic in the sense that they provide a better fit of the experimental data. Consequently, the deflection and the stress field predicted in using the nonlinear models should be closer to the real physical situation than the deflection and the stress field predicted by the models obtained by blind linearization of the nonlinear consitutive relations.

The question we have asked has been whether the quantitative difference between the predictions based on the linearized and nonlinear models could be of importance in practice. We have found that the predictions based on the linearized model can be indeed considerably different from the "correct" predictions based on nonlinear models. This shows that the small strain elasticity is not necessarily tantamout to classical linearized elasticity. The nonlinearity is, contrary to conventional wisdom, of importance even in the small strain range, and plays a significant role not only in the study of new materials such as metallic alloys, but also in the study of ordinary materials such as concrete.

Acknowledgements

References

1. K.R. Rajagopal, *On implicit constitutive theories*, Appl. Math., **48**, no. 4, 279–319, 2003.

2. K.R. Rajagopal, *The elasticity of elasticity*, Z. Angew. Math. Phys., **58**, no. 2, 309–317, 2007.

3. A.D. Freed, D.R. Einstein, *An implicit elastic theory for lung parenchyma*, Int. J. Eng. Sci., **62**, no. 0, 31–47, 2013.

4. A.D. Freed, *Soft Solids*, Modeling and Simulation in Science, Engineering and Technology, Basel: Birkhäuser, 2014, A Primer to the Theoretical Mechanics of Materials.

5. K.R. Rajagopal, *On the nonlinear elastic response of bodies in the small strain range*, Acta Mech., **225**, no. 6, 1545–1553, 2014.

6. Z. Grasley, R. El-Helou, M. D'Ambrosia, D. Mokarem, C. Moen, K.R. Rajagopal, *Model of infinitesimal nonlinear elastic response of concrete subjected to uniaxial compression*, J. Eng. Mech., **141**, no. 7, p. 04015008, 2015.

7. T. Saito, T. Furuta, J.-H. Hwang, S. Kuramoto, K. Nishino, N. Suzuki, R. Chen, A. Yamada, K. Ito, Y. Seno, T. Nonaka, H. Ikehata, N. Nagasako, C. Iwamoto, Y. Ikuhara, T. Sakuma, *Multifunctional alloys obtained via a dislocation-free plastic deformation mechanism*, Science, **300**, no. 5618, 464–467, 2003.

8. S. Kuramoto, T. Furuta, J. Hwang, K. Nishino, T. Saito, *Elastic properties of Gum Metal*, Mater. Sci. Eng. A, **442**, no. 1–2, 454–457, 2006.

9. R. Bustamante, K.R. Rajagopal, *Solutions of some boundary value problems for a new class of elastic bodies undergoing small strains. Comparison with the predictions of the classical theory of linearized elasticity: Part I. Problems with cylindrical symmetry*, Acta Mech., **226**, no. 6, 1815–1838, 2015.

10. S. Timoshenko, J.N. Goodier, *Theory of Elasticity*, 2nd ed., McGraw-Hill Book Company, Inc., New York, Toronto, London, 1951.

11. S.P. Timoshenko, J.M. Gere, *Theory of Elastic Stability*, 2nd ed., Dover, 2009.

12. A.R. Srinivasa, *On a class of Gibbs potential-based nonlinear elastic models with small strains*, Acta Mech., **226**, no. 2, 571–583, 2015.

13. S.M. Han, H. Benaroya, T. Wei, *Dynamics of transversely vibrating beams using four engineering theories*, J. Sound Vib., **225**, no. 5, 935–988, 1999.

14. L.N. Trefethen, *Spectral methods in MATLAB*, Software, Environments, and Tools, **10**, Philadelphia, PA: Society for Industrial and Applied Mathematics (SIAM), 2000.

15. J.A. Weideman, S.C. Reddy, *A MATLAB differentiation matrix suite*, ACM Trans. Math. Softw., **26**, no. 4, 465–519, 2000.

16. W.M. Gentleman, *Implementing Clenshaw–Curtis quadrature, I Methodology and experience*, Commun. ACM, **15**, 337–342, May 1972.

17. W.M. Gentleman, *Implementing Clenshaw–Curtis quadrature, II Computing the cosine transformation*, Commun. ACM, **15**, 343–346, May 1972.

18. G. von Winckel, *Fast Clenshaw–Curtis Quadrature*, MATLAB Central File Exchange, February 2005, http://www.mathworks.com/matlabcentral/fileexchange/6911-fast-clenshaw-curtis-quadrature.

19. J. Waldvogel, *Fast construction of the Fejér and Clenshaw–Curtis quadrature rules*, BIT Numerical Mathematics, **46**, no. 1, 195–202, 2006.